Nuclear Instruments and Methods in Physics Research B 268 (2010) 3186–3190

Contents lists available at ScienceDirect

Nuclear Instruments and Methods in Physics Research B

journal homepage: www.elsevier.com/locate/nimb

Study of defects in implanted silica glass by depth profiling Positron Annihilation Spectroscopy

R.S. Brusa [a,*], S. Mariazzi [a], L. Ravelli [a,c], P. Mazzoldi [b], G. Mattei [b], W. Egger [c], C. Hugenschmidt [d], B. Löwe [d], P. Pikart [d], C. Macchi [e], A. Somoza [e]

[a] CNISM, Dipartimento di Fisica, Università di Trento, Via Sommarive 14, I-38050 Povo, Trento, Italy
[b] CNISM, Dipartimento di Fisica, Università di Padova, Via Marzolo 8, 35131 Padova, Italy
[c] Institut für Angewandte Physik und Messtechnik, Universität der Bunderswehr München, 85577 Neubiberg, Germany
[d] Physik Department E21 and FRMII, Technische Universität München, 85747 Garching, Germany
[e] IFIMAT, UNCentro and CICPBA, Pinto 399, B7000GHG Tandil, Argentina

ARTICLE INFO

Article history:
Received 28 November 2009
Available online 1 June 2010

Keywords:
Silica glass
Positronium
Positrons
Ion implantation

ABSTRACT

Positron Annihilation Spectroscopy (PAS) performed with continuous and pulsed positron beams allows to characterize the size of the intrinsic nano-voids in silica glass, their in depth modification after ion implantation and their decoration by implanted ions. Three complementary PAS techniques, lifetime spectroscopy (LS), Doppler broadening spectroscopy (DBS) and coincidence Doppler broadening spectroscopy (CDBS) will be illustrated by presenting, as a case study, measurements obtained on virgin and gold implanted silica glass.

1. Introduction

PAS is a well established spectroscopy tool for studying open volume defects in all type of materials: metals, semiconductors, polymers [1–3]. It is possible to depth profile from few nm to several microns the samples by tuning positron implantation energy from few eV to about 30 keV. Injected positrons slow down to thermal energy in few picoseconds, then they start a diffusive motion ending their life by annihilation with an electron of the medium. At each implantation energy, a fraction of positrons diffuses at the surface of the sample annihilating in a surface state, a fraction annihilates in a bulk state and a fraction is trapped into open volume defects where it annihilates. Positrons have high sensitivity to single vacancy, vacancy clusters and open volumes up to nano size. They are preferentially trapped in these sites due to the missing positive charge of the ions.

In insulators, when nano or sub-nanovoids are present, positrons can form positronium (Ps) the electron positron bound state. Ps is formed in two spin states. Ortho-positronium (o-Ps, triplet state, total spin number 1, formation probability 3/4) and para-positronium (p-Ps, singlet state, total spin 0, formation probability 1/4). p-Ps has a vacuum lifetime of 125 ps. The p-Ps lifetime in α-SiO_2 was found to be 156 ± 4 ps because the distance between positron and electron becomes larger than that in vacuum due to the screening of the Coulomb interaction with the electrons of the medium [4]. o-Ps has a lifetime of 142 ns in vacuum, but this lifetime is shortened to few nanoseconds in a void of the matter by the so called pick-off process. In the pick-off process the positron of the o-Ps atom, annihilates with an electron of opposite spin of the environment. In fused silica glass up to 80% of positrons form Ps.

Information on open volumes defects (distribution in depth, sizes, decorations) can be obtained by looking at the 511 keV positron–electron annihilation gamma rays and to the positron and positronium lifetime.

In spite of their technological importance [5], silica glasses have not been deeply investigated by PAS [6–9]. Recently, we have started a systematic analysis of silica glass implanted with different ions with the aim of studying the modification of the intrinsic sub-nanovoids of the material and the induced defects [10,11].

In this paper we will present the information that can be obtained by studying virgin and implanted silica glass with three complementary PAS techniques. It will be shown as a full description of the intrinsic sub nanovoids and of the open volume defects can be achieved with these techniques. In Section 3 it will be shown as LS allows the characterization of the type of defects formed by ion implantation. The depth distribution of this defects can be extracted by analyzing the data obtained by the DBS technique, Section 4. And finally, in Section 5, the presence of gold associated to some defects is outlined. To this aim, the sensitivity of the CDBS technique to the chemical environment around open volume defects is used.

* Corresponding author. Tel.: +39 0461 881552; fax: +39 39 0461 881696.
E-mail address: brusa@science.unitn.it (R.S. Brusa).

0168-583X/$ - see front matter © 2010 Elsevier B.V. All rights reserved.
doi:10.1016/j.nimb.2010.05.084

2. Samples

Samples were obtained from silica glass slabs (Herasil 1 by Heraeus) produced by fusion of natural quartz crystals. Slabs were implanted at room temperature with a 200 kV high-current implanter (Danfysik 1090) at the INFM-INFN Ion Implantation Laboratory (Legnaro, Italy). Au^+ ions at 190 keV were implanted in the silica slab with a fluence of 5×10^{14} ions/cm^2. To avoid sample heating during implantation the ion flux was maintained at 0.1 μA/cm^2. The ion projected range R_p, calculated by using SRIM program [12], was $R_p = 67$ nm with a straggling $\Delta R_p = 14$ nm.

3. Lifetime Spectroscopy (LS)

LS allows the characterization of defect types and the dimension of intrinsic sub nanovoids in silica glass. The positron lifetime measurements were done with the apparatus PLEPS (Pulsed Low Energy Positron Beam) [13] at the high intense positron source NEPOMUC (Neutron induced POsitron source MUniCh) [14]. An example of a measured lifetime spectrum is plotted in Fig. 1. The lifetime spectrum $F(t)$ is a sum of exponential decay lifetime components:

$$F(t) = \sum_i^N \frac{I_i}{\tau_i} \exp\left(-\frac{t}{\tau_i}\right) \quad (1)$$

where τ_i and I_i are the positron lifetime in the state i and its associate intensity, respectively. The positron lifetime is inversely proportional to the local electron density in the annihilation site [1,3]. As a consequence, lifetime values increase when positrons become trapped in larger open volumes. When the open volume reaches the sub-nanometer size, Ps can be formed [1–3]. In materials similar to those studied in the present work, from the decomposition of the LS spectra, up to four components representing different annihilation sites can be well-resolved.

For this experiment, lifetime spectra were acquired in the 0.5–18 keV positron implantation energy range and analyzed by POSFIT. The overall (detector plus pulsing system) time resolution was 280 ps. At each energy from 3 to 5 millions counts were acquired with a counting rate of 8000 counts per second. A lifetime depth profiling with 15 positron implantation energies requires a measurement time from 3 to 4 h. From the analysis of the spectra, three lifetime components were enough to obtain good fits of the experimental data.

According to the Makhovian implantation profile, the mean positron implantation depth $\bar{z}$ in nanometers is related to the positron implantation energy E by the equation $\bar{z} = (40/\rho)E^{1.6}$ when the material density ρ (2.3 g/cm^3 for fused silica glass) and energy E are expressed in g/cm^3 and keV, respectively [1–3].

The lifetimes and the respective intensities as obtained by measuring the Au implanted sample are shown in Fig. 2 and Fig. 3 as a function of the positron implantation energy. The damage region extends from the surface to about 300 nm depth (see DBS measurements in the next paragraph) corresponding to a positron implantation energy of about 6 keV. For energies above 12 keV positrons are implanted beyond 1 μm depth and annihilate in the bulk of silica glass. Therefore the measurements above 12 keV positron implantation energy characterize the virgin silica and will be discussed in advance.

The longest lifetime ($\tau_3 \approx 1600$ ps, $I_3 \approx 57\%$) is due to o-Ps pick-off annihilation in the intrinsic sub-nanovoids of the silica. The pick-off reduced o-Ps lifetime is correlated to the size of the open voids in which o-Ps annihilate. An estimation of the dimension of the open volume in silica can be obtained by the Tao-Eldrup semi-empirical model that relates the pick-off reduced o-Ps lifetime to

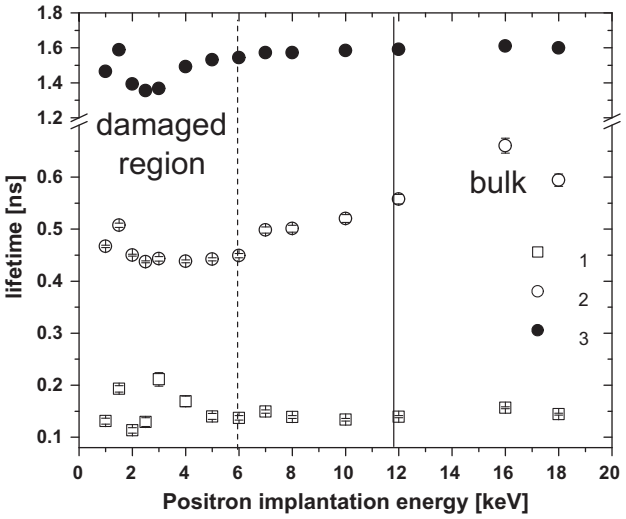

Fig. 2. Positron lifetimes as a function of the positron implantation energy. The longest lifetime τ_3 corresponds to the o-Ps pick-off annihilation. The dashed vertical line marks the damage region by Au^+ implantation. The continuous vertical line marks the bulk of the unaffected silica glass.

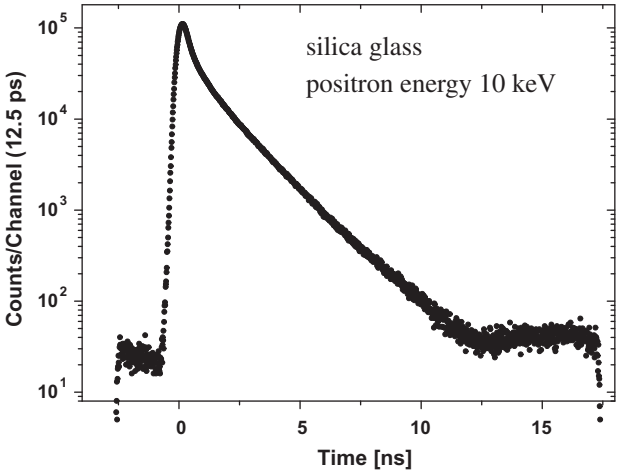

Fig. 1. Typical lifetime spectra. The long decaying exponential is due to o-Ps pick-off annihilations.

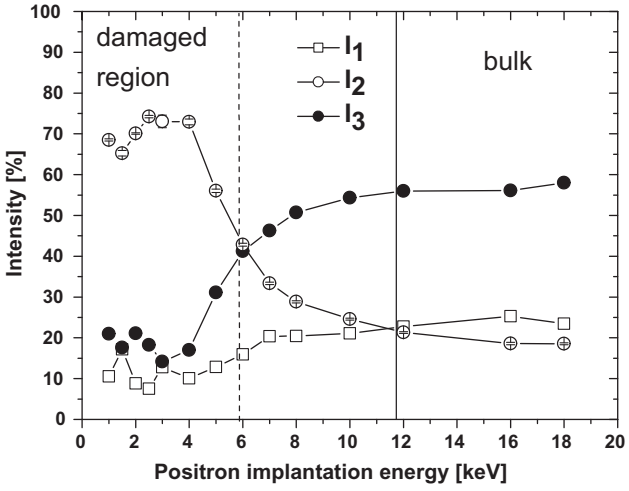

Fig. 3. Positron intensities of the respective lifetimes as a function of the positron implantation energy. The dashed vertical line marks the damage region by Au^+ implantation. The continuous vertical line marks the bulk of unaffected silica glass.

the average sizes of the free open volume [15–17]. The cavity hosting Ps is assumed to be a spherical void with effective radius R. Such a Ps trap has a potential well with finite depth; however, for convenience of calculations one usually assumes the depth as infinite, but the radius increased to $R+\Delta R$, ΔR (0.166 nm) being an empirical parameter which describes the penetration of Ps wave function into the bulk [17]. The electron density is supposed to be zero for $r < R$ and constant for $r > R$. The relationship between o-Ps lifetime τ_3 (ns) and radius R is the following:

$$\tau_3 = 0.5\left[\frac{\Delta R}{R+\Delta R}+\frac{1}{2\pi}\sin\left(2\pi\frac{R}{R+\Delta R}\right)\right]^{-1} \quad (2)$$

Of course, the values of the radii obtained from Eq. (3) should be interpreted only as rough estimates, since real voids are irregularly shaped.

In the present sample, Herasil 1, with an o-Ps lifetime of 1.6 ns, the size of the intrinsic sub-nanovoids with diameter d is found to be 0.5 nm from Eq. (3). The dimension of the voids as a function of the silica content was studied in several glasses by Sasaki et al. [9].

The second lifetime ($\tau_2 \approx 600$ ps, $I_2 \approx 19\%$) is attributed to annihilation of trapped positrons [8]. It is important to note that both trapped positrons and positrons of o-Ps annihilate with the oxygen atoms decorating the walls of the sub-nanovoids. In our fused silica sample about 76% of implanted positrons are found to form Ps (4/3 I_3). Fast positron annihilations and p-Ps annihilations contribute to the shortest lifetime ($\tau_1 \approx 150$ ps, $I_1 \approx 24\%$).

As mentioned above, in the samples studied in the present work, ion implantation produces damage from the surface up to 300 nm depth. In this damage region (see Fig. 3) a strong quenching of Ps formation is observed: the intensity I_3 drops from 57% to 20% and I_1 from 24% to 10%. This reduction can be due to concomitant factors: compacting of the material with reduction of free volumes available for Ps formation, enrichment of the free volumes by displaced oxygen, free electrons at dangling bonds. Conversely the fraction I_2 increases from 19% up to 73%. The strong increase of I_2 is due to the oxygen enrichment of the trapping sites and annihilation of positrons at negative charged oxygen-related defects as evidenced by the decrease of the lifetime τ_2 of the trapped positrons to $\tau_2 \approx 450$ ps (Fig. 2). The reduction from 600 to 450 ps of τ_2 is associated at the presence of O_2^- defects [8]. The slight increase of the shortest lifetime τ_1 over 150 ps is associated to the presence of nonbridging oxygen hole centers $\equiv$Si–O$^-$ [8].

Summarizing, LS measurements show that in the first 300 nm (corresponding to a positron implantation energy of about 6 keV) of the silica glass most of the intrinsic sub nanovoids are both compacted and filled by oxygen atoms. Many of this oxygen atoms are expected to be negatively charged. The o-Ps pick-off lifetime τ_3 that decreases to about 1400 ps points out a reduction in size of the remaining sub-nanovoids ($d \approx 0.45$ nm).

The monotonically variation of the lifetimes and their intensities between ~4 keV and 12 keV is due to the positrons diffusion length. In this region positrons diffusing in the bulk silica glass probe both the bulk and the defected region (see next paragraph).

4. Doppler Broadening Spectroscopy (DBS)

The defects distribution can be obtained by the analysis of the DBS measurements. With depth profiling DBS technique the 511 keV positron-electron annihilation line is measured at different positron implantation energy. The broadening of the line is evaluated by the so called S parameter defined as the ratio between the counts in a central area and the counts in the total area of the annihilation peak (see Fig. 4). The electron momentum component p_L in the detector direction is related to the energy shift $\Delta E = |E_\gamma - 511\ \text{keV}|$, where E_γ is the energy of the detected gamma ray, by the equation: $p_L = \frac{2\Delta E}{c}$. Hence, the S parameter is an indication of positron annihilation with low momentum electrons.

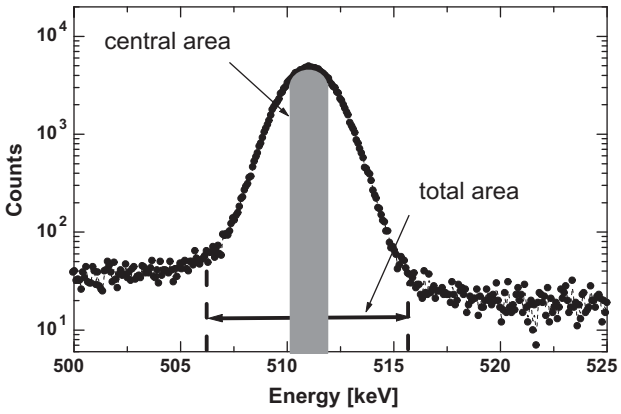

Fig. 4. Annihilation line (511 keV). The total and central areas of the peak used to define the S parameter are highlighted.

The S parameter as a function of the positron implantation energy, as measured by the Trento continuous slow positron beam [18], is reported in Fig. 5 for the virgin and the Au implanted sample. The measured $S(E)$ parameter values were normalized to the $S_{Si} = 0.537$ parameter measured in the bulk of a p-type (1 0 0) Si single-crystal. This choice allows the comparison with data on silica samples obtained in other laboratories [2]. For each energy, about 3×10^5 counts were accumulated under the 511 keV line, corresponding to an error of 1×10^{-3} on the S parameter.

Each $S(E)$ measured in the virgin sample is a linear combination of the $S_b(E > 12\,\text{keV})$ and $S_s(E \to 0)$ characteristic of positron annihilation in the silica bulk and at the silica surface, respectively:

$$S(E) = S_b f_b(E) + S_s f_s(E) \quad (3)$$

where $f_b(E), f_s(E)$ are the fractions of positron annihilating in the bulk and surface states. The measured S values increase monotonically from the S_s to the S_b.

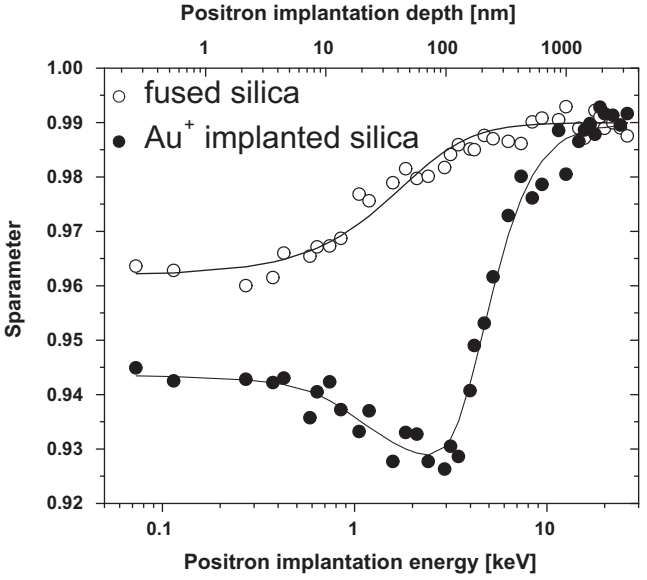

Fig. 5. S parameter, normalized to bulk silicon, as a function of positron implantation energy (lower scale) and mean positron implantation depth (upper scale) for fused silica and Au$^+$ implanted silica glass. The solid lines are best fit to the experimental data using the positron stationary diffusion equation.

The ion implantation produce a strong decrease in the S parameter values (see Fig. 5). The $S(E)$ parameter shows a well pronounced minimum and a subsequent increase, reaching the S_b bulk value. The broadening of the annihilation line produced by irradiation is related to the different and coexistent phenomena pointed out by lifetime measurements. The compacting of the material and the filling of sub-nanovoids with oxygen atoms reduce the free volumes available for Ps formation: this also means a less p-Ps contribution to the narrowing of the 511 keV annihilation line. The oxygen enrichment of the free volumes increases the positron annihilation with oxygen electrons that contribute to the broadening of the annihilation line [2].

The $S(E)$ in the implanted sample can be described by a linear combination taking into account positron trapping into defects:

$$S(E) = S_b f_b(E) + S_s f_s(E) + \sum_i S_{di} f_{di}(E) \tag{4}$$

where S_{di} and $f_{di}(E)$ are the characteristic S parameter of the defect of type i and the fraction of positron annihilating in the defect i.

Modeling the $S(E)$ curves by the positron stationary diffusion equation (Eq. (5)) allows to extract the distribution of the defect profiles [19]. The positron density $n(z,E)$ is the solution of the positron diffusion equation:

$$D^+ \frac{\partial^2 n(z,E)}{\partial z^2} - \left[\lambda_b + \sum v_i C_i(z)\right] n(z,E) + P(z,E) = 0 \tag{5}$$

D^+ is the positron diffusion constant, λ_b the positron annihilation rate in silica (taken as the inverse of the mean lifetime in the bulk $\lambda_b = 1/1060\ \mathrm{ps}^{-1}$) and v_i the specific trapping rate per unit defect concentration. The positron implantation profile $P(z,E)$ [1–3] is given as input while the functional forms of the defect profile $C_i(z)$ are inserted as a guess. v_i is a fitting parameter. The fraction $f_b(E), f_s(E), f_{di}(E)$ are related to the positron density $n(z,E)$ by the equations:

$$\begin{aligned} f_b &= \lambda_b \int_0^\infty n(z,E)\,dz \\ f_s &= D_+ \left[\frac{dn(z,E)}{dz}\right]_{z=0} \\ f_{di} &= v_i \int_0^\infty C_i(z) n(z,E)\,dz \end{aligned} \tag{6}$$

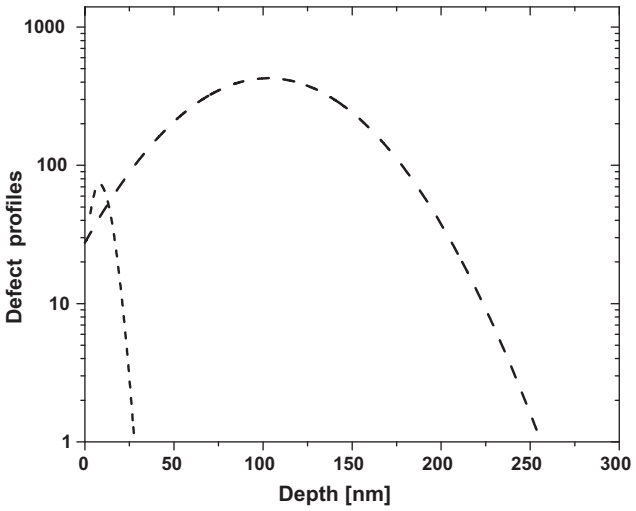

Fig. 7. Defect distribution as a function of depth as obtained by fitting the experimental data of Fig. 5 using the positron stationary diffusion equation.

The obtained fraction $f_b(E), f_s(E), f_{di}(E)$ and the extracted defect profiles are shown in Figs. 6 and 7 respectively. The continuous lines in Fig. 5 are the best fit to the $S(E)$ curves with the data of Figs. 6 and 7. The positron diffusion length in the virgin sample was found to be $L_+ = 48$ nm. Two defect distributions are pointed out in the implanted sample: the first one very near to the surface, the second one extending very deeply in the sample. The first distribution is confined in a region (<40 nm; <2 keV) below the R_p. In this region there is a slightly reduction of oxygen filling nanovoids and oxygen-related defects (see decrease of I_2 in Fig. 3). The defects in the second distribution reach a depth of about four times the R_p. These defects are oxygen filling the nanovoids and negatively charged oxygen defects (see LS measurements). Probably, to reach this depth, the mobility of displaced oxygen atoms is increased by the stress field which is known to be produced by volumetric change on the surface of insulators after implantation [20].

The functional forms adopted as a guess were a derivative of a Gaussian and a Gaussian for the first and the second defect distribution, respectively.

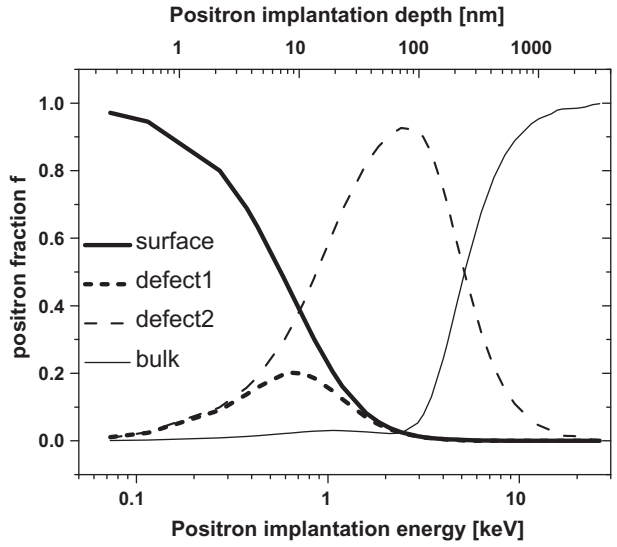

Fig. 6. Fractions of positron annihilating in the different annihilation states: surface, bulk, two types of defects.

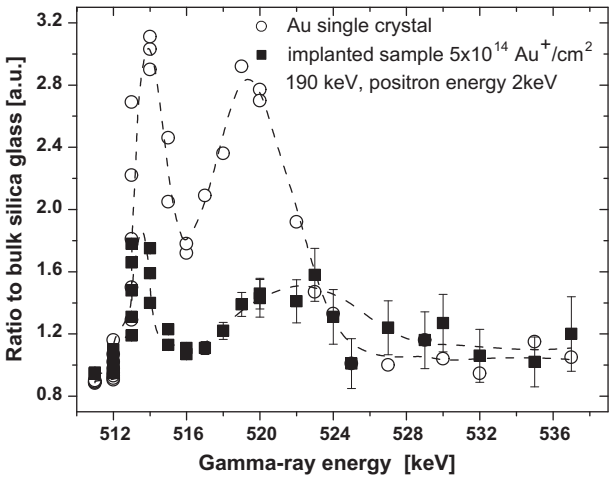

Fig. 8. CDBS measurements. Ratio of the Au single crystal and of the Au implanted silica glass 511 keV annihilation line to the 511 keV annihilation line of silica glass. The spectrum of the Au implanted silica glass was measured at 2 keV positron implantation energy. The dashed lines are a guide to the eyes.

5. Coincidence Doppler Broadening Spectroscopy (C-DBS)

Positrons annihilation with high momentum electrons, i.e. the outermost core electrons of the atoms, populate the tail of the 511 keV annihilation line. As the core electrons maintain their atomic characteristic also in a solid [21,22], the signal from positron-core electron annihilation can be used to have information on the chemical species surrounding the annihilation site [23,24]. The annihilation probability with these electrons is very low because positrons are repelled by the ion core and the signal is comparable with the background. To extract the information a background reduction coincidence technique with two germanium detector must be used and usually 2×10^7 counts or more must be recorded in coincidence. The coincidence measurements were done at the high intense positron source NEPOMUC [14,25] with a resolution in coincidence of 1.1 keV at 511 keV. To highlight the fingerprint signal coming from the atom around the annihilation site, the data are presented as ratio curve respect with a reference sample. In the present measurements as a reference a coincidence curve measured in the bulk of a silica glass sample was used. A gold single crystal was also measured to mark the characteristic feature of this element in the high momentum annihilation region. In Fig. 8 the measured 511 keV annihilation lines in pure Au and in the Au implanted silica are reported as ratio to the 511 keV annihilation line in bulk silica glass. The spectrum of Au implanted silica was measured at 2 keV positron implantation energy. This energy correspond to a depth of 53 nm, and hence very near to the R_p. As can be seen in Fig. 8, the Au ratio curve shows two well defined peaks centered at gamma energy E_γ around 513.5 and 519.0 keV. A peak at about 519 keV is present also in CDBS measurements on SiO_2 and Si surfaces [26] and there was attributed to annihilation with oxygen. In the Au implanted silica glass the two peaks are also present with the second one slightly shifted to higher gamma energies ($\sim$521 keV). This is an indication that some positrons traps are near to the Au implanted atoms, the shift in the second peak could be due to the simultaneous presence of Au and oxygen near to the positron trap. A more quantitative discussion would require of theoretical calculations [27] and the consideration of contribution of the different positron annihilation states to the measured spectrum [23,24].

6. Conclusions

It was shown that, using three complementary PAS techniques, information on the intrinsic dimension of sub nanovoids of silica glass and on the type and distribution of defects produced by ion implantation can be obtained. At present, these measurements can be carried out in relatively short times at the NEPOMUC facility. Many properties of silica glass materials depend from its morphology, doping and silica content. Non destructive methods, like PAS, to characterize open volumes and their decoration in insulators, can have an important role due to the wide use of silica glass based materials in several technological field, from optical to housing and mechanical. Theoretical works are necessary to extract quantitative information on the decoration of defects from CDBS measurements.

References

[1] A. Dupasquier, A.P. Mills, Jr. (Eds.), Positron Spectroscopy of Solids, North-Holland, Amsterdam, 1995.
[2] P. Asoka-Kumar, K.G. Lynn, D.O. Welch, J. Appl. Phys. 76 (1994) 4935–4982.
[3] R. Krause-Rehberg, H.S. Leipner, Positron Annihilation in Semiconductors, Defect Studies, Springer Series in Solid State Science, Springler-Verlag, Berlin, Heidelberg, 1999.
[4] H. Saito, T. Hyodo, Phys. Rev. Lett. 90 (2003) 193401–193404.
[5] P. Mazzoldi, G. Mattei, in: B. Corain, G. Schmid, N. Toshima (Eds.), Metal Nanoclusters in Catalysis, Materials Science the Issue of Size-control, Elsevier, Amsterdam, 2007, p. 281.
[6] Z. Zuh, Y. Jin, C. Li, Y. Sun, C. Zhang, Q. Meng, Nucl. Instrum. Methods Phys. Res. B 146 (1998) 455– 461.
[7] C. Hugenschmidt, U. Holzwarth, M. Jansen, S. Kohn, K. Maier, J. Non-Cryst. Sol. 217 (1997) 72–78.
[8] M. Hasegawa, M. Saneyasu, M. Tabata, Z. Tang, Y. Nagai, T. Chiba, Y. Ito, Nucl. Instrum. Methods Phys. Res. B 166–167 (2000) 431–439.
[9] Y. Sasaki, Y. Nagay, H. Ohkubo, K. Inoue, Z. Tang, M. Hasegawa, Rad. Phys. Chem. 68 (2003) 569–572.
[10] P. Mazzoldi, G. Mattei, S. Mariazzi, R.S. Brusa, Radiat. Effects Defects Solids 164 (2009) 1–7.
[11] P. Mazzoldi, G. Mattei, L. Ravelli, W. Egger, S. Mariazzi, R.S. Brusa, J. Phys. D: Appl. Phys. 42 (2009) 115418–115426.
[12] J.P. Biersack, L. Haggmark, Nucl. Instr. Meth. 174 (1980) 257. SRIM code at <www.srim.org>.
[13] P. Sperr, W. Egger, G. Kögel, G. Dollinger, C. Hugenschmidt, R. Repper, C. Piochacz, Appl. Surf. Sci. 255 (2008) 35–38.
[14] C. Hugenschmidt, G. Dollinger, W. Egger, G. Kögel, B. Löwe, J. Mayer, P. Pikart, C. Piochacz, R. Repper, K. Schreckenbach, P. Sperr, M. Stadlbauer, Appl. Surf. Sci. 255 (2008) 29–32.
[15] M. Eldrup, in: P.G. Coleman, S.C. Sharma, L.M. Diana (Eds.), Positron Annihilation, North Holland, Amsterdam, 1982, pp. 753–772.
[16] S.J. Tao, J. Chem. Phys. 56 (1972) 5499–5510.
[17] M. Eldrup, D. Lightbody, N. Sherwood, J. Chem. Phys. 63 (1981) 51–58.
[18] A. Zecca, M. Bettonte, J. Paridaens, G.P. Karwasz, R.S. Brusa, Measur. Sci. Technol. 9 (1998) 409–416.
[19] R.S. Brusa, G.P. Karwasz, N. Tiengo, A. Zecca, F. Corni, G. Ottaviani, R. Tonini, Phys. Rev. B 61 (2000) 10154–10166.
[20] G. Battaglin, G.W. Arnold, G. Mattei, P. Mazzoldi, J.-C. Dran, J. Appl. Phys. 85 (1999) 8040–8049.
[21] P. Asoka-Kumar, M. Alatalo, V.J. Ghosh, A.C. Kruseman, B. Nielsen, K.G. Lynn, Phys. Rev. Lett. 77 (1996) 2097–2100.
[22] R.S. Brusa, W. Deng, G.P. Karwas, A. Zecca, Nucl. Instrum. Meth. B 194 (2002) 519–531.
[23] C. Macchi, S. Mariazzi, G.P. Karwasz, R.S. Brusa, P. Folegati, S. Fabbroni, G. Ottaviani, Phys. Rev. B 74 (2006) 174120–174212.
[24] R.S. Brusa, Phys. Status Solidi (C) 10 (2007) 3614–3619.
[25] C. Hugenschmidt, B. Löwe, J. Mayer, C. Piochacz, P. Pikart, R. Repper, M. Stadlbauer, K. Schreckenbach, Nucl. Instrum. Methods A 593 (2008) 616–618.
[26] C. Hugenschmidt, P. Pikart, K. Schreckenbach, Phys. Status Solidi C 6 (2009) 2459–2461.
[27] M. Alatalo, B. Barbiellini, M. Hakala, H. Kauppinen, T. Korhonen, M.J. Puska, K. Saarinen, P. Hautojärvi, R.M. Nieminen, Phys. Rev. B 54 (1996) 2397–2409.